



# Structure-based design, synthesis and evaluation of 2,4-diaminopyrimidine derivatives as novel caspase-1 inhibitors

Shivani Patel<sup>a,b</sup>, Palmi Modi<sup>a</sup>, Vishal Ranjan<sup>c</sup>, Mahesh Chhabria<sup>a,\*</sup>

<sup>a</sup> Department of Pharmaceutical Chemistry, L.M. College of Pharmacy, Navrangpura, Ahmedabad 380009, Gujarat, India

<sup>b</sup> Division of Biological and Life Sciences, Ahmedabad University, Ahmedabad 380009, Gujarat, India

<sup>c</sup> Oxygen Healthcare Research Pvt. Ltd. Changodar, Ahmedabad 382213, Gujarat, India

## ARTICLE INFO

### Article history:

Received 1 December 2017

Revised 12 March 2018

Accepted 18 March 2018

Available online 27 March 2018

### Keywords:

Interleukin-1 $\beta$  converting enzyme

Cytokine

Structure based design

2,4-Diaminopyrimidine

Anti-inflammatory agent

## ABSTRACT

Interleukin-1 $\beta$  converting enzyme contributes in various inflammatory and autoimmune diseases by maturing pro-inflammatory cytokines IL-1 $\beta$ , IL-18 and IL-33. Therefore, inhibition caspase-1 may provide a potential therapeutic strategy for the treatment of chronic inflammatory diseases. Here we have reported structure-based design, synthesis and biological evaluation of 2,4-diaminopyrimidine derivatives (**6a-6w**) as potential caspase-1 inhibitors. Six compounds **6m**, **6n**, **6o**, **6p**, **6q** and **6r** showed significant enzymatic inhibition with IC<sub>50</sub> ranging from 0.022 to 0.078  $\mu$ M. These compounds also displayed excellent cellular potency at sub-micromolar concentration. Moreover, molecular docking studies provided the useful binding insights specific for caspase-1 inhibition. All these results indicated that compounds **6m**, **6n** and **6o** could be potential leads for the development of newer caspase-1 inhibitors as anti-inflammatory agents.

© 2018 Elsevier Inc. All rights reserved.

## 1. Introduction

Caspases are cysteine-dependent aspartate-specific proteases, primarily responsible for proinflammatory cytokine maturation and apoptosis. These endoproteases possess cysteine as a nucleophile for hydrolysing peptide bonds that occurs mainly after C-terminus of Asp residues [1]. Fourteen human caspases have been identified and classified based on their biological functions and length of regulatory pro-domains: (I) Inflammatory caspases (Caspases-1, 4, 5 and 11), (II) Initiator caspases (Caspases-2, 8, 9, 10 and 12) and (III) Effector caspases (Caspases-3, 6, 7 and 14) [2,3]. Generally, they exist as inactive precursors which acquired enzymatic activity by auto activation or by amplification cascade, a highly regulated process. The active caspase is homodimer of heterodimers (containing p10 and p20 subunits) with two active sites located in close proximity model.

Interleukin-1 $\beta$ -converting enzyme (ICE, caspase-1) is mainly responsible for post-translational processing of the pro-inflammatory cytokines such as IL-1 $\beta$ , IL-18 and IL-33. The biologically inactive pro-IL-1 $\beta$  (31 kDa) undergoes proteolytic cleavage at Asp<sup>116</sup>-Ala<sup>117</sup> which, releases the mature cytokine, IL-1 $\beta$  (17.5 kDa) [4]. IL-1 $\beta$  plays a key role in physiological process such as

inflammation, cell proliferation, differentiation and pyroptosis. Excessive secretion of IL-1 $\beta$  contributes to the pathophysiology of various inflammatory and autoimmune diseases such as rheumatoid arthritis (RA), osteoarthritis (OA), atherosclerosis and sepsis [5]. Literature also reveals that caspase-1 might be involved in unscheduled programmed cell death in many degenerative diseases [6]. As the key component of inflammation induction, caspase-1 has emerged as an important therapeutic target for modulating various inflammatory diseases.

Large numbers of anti-inflammatory drugs only improve the disease related symptoms and show side effects of NSAIDs [7]. Currently used IL-1 receptor antagonist (Kineret) or anti-IL-1 $\beta$  antibody (canakinumab) also exhibit some severe allergic reactions [8,9]. A positional scanning library identifies Ac-YVAD-CHO, tetrapeptide fragment as a potent, selective caspase-1 inhibitor (Ki 5 nM) [10]. Unfortunately, this peptide suffers from poor pharmacokinetic profile and modest selectivity within the enzyme family. Based on these requisites, two peptidomimetics VX-740 (pralnacasan) and VX-765 were developed and progressed into late-stage of clinical trials [11,12]. However, several pharmacological constrain limits their clinical utility. Thus, ICE represents an opportunity for the development of small molecules as novel anti-inflammatory agents.

The X-ray crystal structure of caspase-1 and their subsequent peptide inhibitors provided clear premises for structure based design of newer caspase-1 inhibitors [13]. Further the molecular

\* Corresponding author.

E-mail address: [mahesh.chhabria@rediffmail.com](mailto:mahesh.chhabria@rediffmail.com) (M. Chhabria).

docking study revealed the key residual interactions, which includes polar interactions with Arg179, His237 and Cys285 at P1site; H-bonding interactions with Ser339 and Arg341 at P2-P3 site and hydrophobic interactions with Trp 340, His342, Pro343 and Arg383 at P4 site. A summary of the protein-ligand interactions of co-crystallized ligand and 6 m with 1rx is displayed in Fig. 1. It clearly emphasized that both compounds occupy the same spatial area and position in to the binding site of caspase-1. Based on these computational results newer series of 2,4-diaminopyrimidine was designed, synthesized and tested against caspase-1 enzyme. Further, the cellular potency of the most active compounds was determined by THP-1 cell based assay.

## 2. Results and discussion

### 2.1. Chemistry

The synthesis of targeted compounds **6a-6w** was accomplished by the synthetic route outlined in Scheme 1. The cyclocondensation of guanidine hydrochloride (**1**) and ethyl acetoacetate (**2**) afforded 2-amino 4-hydroxy 6-methyl pyrimidine (**3**) which was heated with phosphorus oxychloride to get the key intermediate 2-amino-4-chloro-6-methyl pyrimidine (**4**) [14,15]. Compound (**4**) was refluxed with various substituted amines in the presence of catalytic conc. HCl in ethanol to yield compounds (**5a-i**) [16,17]. Finally, 2-amino-(4-substituted phenylamino)-6-methylpyrimidins (**5a-i**) were reacted with substituted phenoxy acetyl chloride in dry DMF gave targeted compounds (**6a-6w**). All the final compounds were characterized by IR, MS, <sup>1</sup>HNMR and <sup>13</sup>C NMR spectroscopic techniques.

### 2.2. Caspase-1 enzyme assay

The synthesized compounds were evaluated for their caspase-1 inhibition potential using luminescence based assay [18]. Compounds were tested in three different concentrations, in comparison to Ac-YVAD-CHO peptide as a standard drug. The Z-WEHD-AMC was used as a substrate and enzyme concentration was adjusted at one unit for catalysing the peptide bond. As shown in Table 1, compounds demonstrated good inhibitory potential with various substituents at both phenyl rings, IC<sub>50</sub> range from 0.022 to 12.48 μM. Firstly, un-substituted phenoxy acetamide (**6a**, IC<sub>50</sub> = 12.48 ± 0.08 μM) was evaluated for its less potency compared to -CH<sub>3</sub> substituted derivatives (**6b**, **6c**, IC<sub>50</sub> = 4.83 ± 0.05,

4.51 ± 0.14 μM). Compound bearing electron withdrawing substituent at R<sub>1</sub> ring (**6d**, IC<sub>50</sub> = 1.86 ± 0.77 μM) showed improved enzymatic inhibition. However, *p*-CH<sub>3</sub> (**6e**, IC<sub>50</sub> = 8.25 ± 0.06 μM) and *p*-OCH<sub>3</sub> (**6f**, IC<sub>50</sub> = 8.73 ± 0.15 μM) substituents at R phenyl showed dramatic loss in the potency. When the R ring was fixed with *p*-methyl/methoxy and R<sub>1</sub> phenyl ring substituted with *o*/*m*-CH<sub>3</sub> group (**6g**, **6h**, IC<sub>50</sub> = 3.78 ± 0.21, 3.56 ± 0.77 μM) displayed 2 fold more potency compare to *p*-CH<sub>3</sub> derivative (**6i**, IC<sub>50</sub> = 6.85 ± 0.08 μM). Replacement of methyl group with *p*-Cl and *p*-F substituents at R<sub>1</sub> phenyl ring showed 4 fold increase in the activity compare to **6i** (**6j**, **6k**, IC<sub>50</sub> = 1.65 ± 0.16 μM, 1.72 ± 0.12 μM). However, 3-Cl, 4-CH<sub>3</sub> substituents at R1 ring did not produce any improvement in the activity (**6l**, IC<sub>50</sub> = 2.80 ± 0.20 μM). The electron withdrawing substituents at remote R phenyl ring demonstrated highest enzymatic inhibition (**6m**, **6n**, **6o**, IC<sub>50</sub> = 0.035 ± 0.007, 0.027 ± 0.005, 0.022 ± 0.013 μM). Incorporation of alkyl substituent at various positions of R1 phenyl also exhibited comparable potency with **6m-6o** (**6p**, **6q**, **6r**, IC<sub>50</sub> = 0.078 ± 0.015, 0.052 ± 0.008 & 0.045 ± 0.010 μM). Whereas, the electronegative substituents at *para* position of both the phenyl ring caused decrease in the activity (**6s**, IC<sub>50</sub> = 1.75 ± 0.21 μM). Specifically, adding the *m*-CH<sub>3</sub> on R<sub>1</sub> and *o*-F substituent on R ring exhibited 2 fold increase in the potency (**6t**, IC<sub>50</sub> = 0.95 ± 0.13 μM). Likewise, 2,3-dimethyl substituents on R phenyl ring led to more than 10 fold decrease in the activity. (**6u**, **6v**, **6w**, IC<sub>50</sub> = 10.57 ± 0.19, 10.81 ± 0.54, 9.78 ± 0.30 μM). These results suggested electron withdrawing substituents at the *para* position of R phenyl and *o*/*m*-CH<sub>3</sub> substituent at R1 phenyl ring influence the activity.

### 2.3. Cell based assay

Compounds exhibiting significant enzymatic inhibition were also evaluated for their cellular potency [19]. As shown in Table 2, most of the compounds displayed comparable cellular potency to the Ac-YVAD-CHO and MG-132. Compound having halogen substituent at *para* position of R phenyl ring (**6m**, IC<sub>50</sub> = 6.25 ± 0.06 μM) showed 2 fold decrease in the potency compare to *ortho* and *meta* positions (**6n**, **6o**, IC<sub>50</sub> = 3.55 ± 0.02, 3.20 ± 0.15 μM). The *o*/*m*-CH<sub>3</sub> substituent on R<sub>1</sub> phenyl (**6q**, **6r** IC<sub>50</sub> = 6.84 ± 0.16, 6.37 ± 0.21 μM) was more tolerated than *p*-CH<sub>3</sub> substituent (**6p**, IC<sub>50</sub> = 8.0 ± 0.3 μM). This, poor correlation between enzymatic and cell-based activity is major concern in discovery of newer caspase-1 inhibitors with important therapeutic potential.

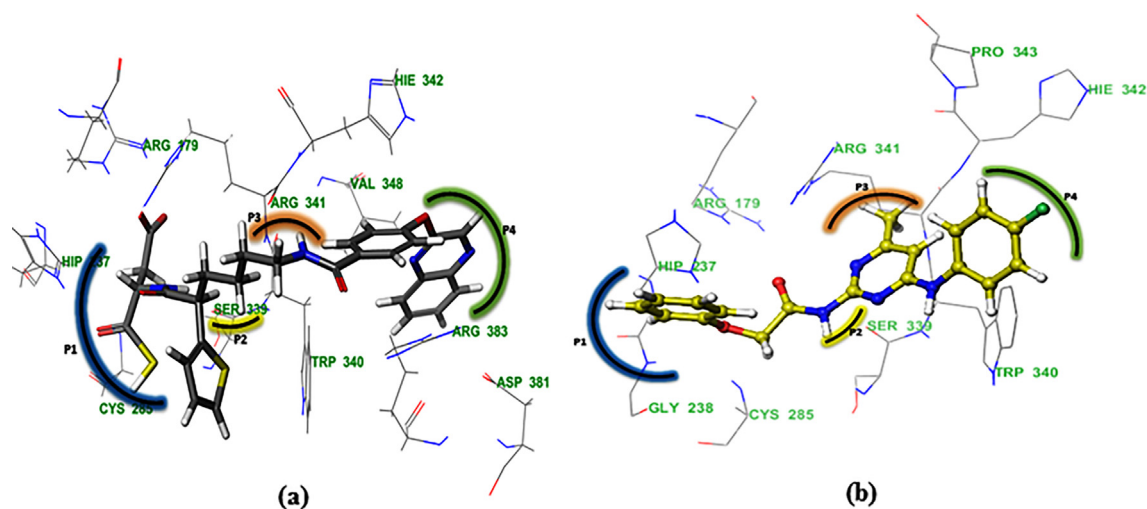
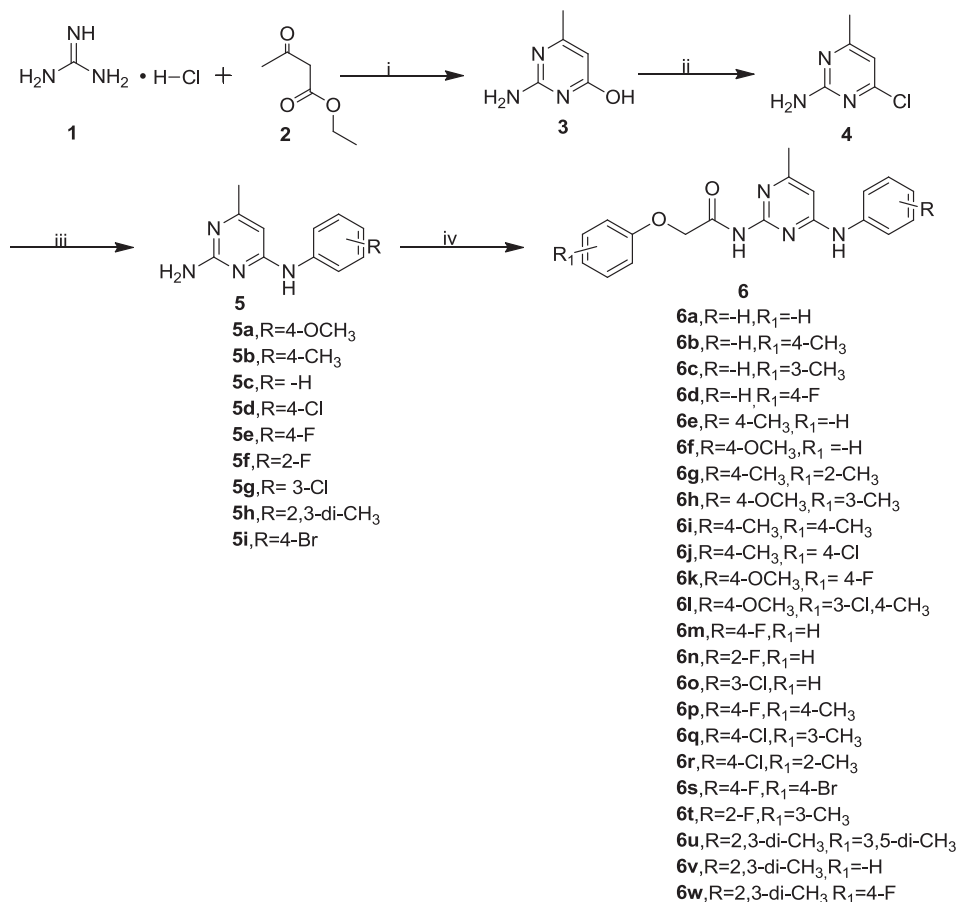


Fig. 1. (a) The key residual interactions of 1rx with co-crystallized ligand (b) The key residual interactions of 1rx with 6 m.



**Scheme 1.** Reagents and conditions: (i) EtOH, NaOH, 3 h, rt; (ii) POCl<sub>3</sub>, PhMe, 30–40 min, 110 °C; (iii) Substituted amines, EtOH, Conc. HCl, 3–4 h, 40 °C; (iv) Substituted Phenoxy acetyl chlorides, Et<sub>3</sub>N, DMF, 1 h, rt.

#### 2.4. Molecular docking studies

In order to gain binding insights comparative docking study was performed using caspase-1, 3, 7 and 8 (PDB ID: 1RWX, 1PAU, 2QL9 and 1F9E) [20]. The proposed binding modes of compounds **6p**, **6m**, **6a** and **6n** and corresponding co-crystal ligands are shown in Figs. 2, 4, 5 and 6. All the compounds were bound in the same region as that of the co-crystal ligand. Compounds exhibited binding energy of –7.508 to –11.260 kcal/M for caspase-1, while the lower binding energy of –1.518 to –4.969 kcal/M for caspase-3, 7 and 8 (Table S1: see supplementary material). Further, to verify these binding interactions **MG-132** and **AC-YVAD-CHO**, reported caspase-1 inhibitors were docked in to the active site of caspase-1 enzyme. The binding poses of these compounds with caspase-1 are shown in Fig. 3. Both the inhibitors formed electrostatic contacts with Arg179 and Arg341; H-bonding interactions with His237, Cys285, Ser339 and Arg341 at P1-P2 site;  $\pi$ - $\pi$  interactions with Trp340, His342, Pro343 and Arg383 residues at the P3-P4 site of caspase-1 protein. Compound **6p** interacted with Arg179, His237, Cys285, Ser339, Trp340, Arg341, His342, Pro343 and Arg383 residues same as reported for caspase-1 inhibitors.

Compound **6m** exhibited polar interactions with Arg179, Arg341 and Gln283 at P1 site; nonpolar interactions with Ser180, Phe256 and Ser339 at the P2 pocket of 1PAU. It also exhibited  $\pi$ - $\pi$  interaction with Trp340 and Arg341 residues at P3 site. The P4 site contained Ser381A mainly formed polar contacts which stabilize the ligand binding.

Compound **6a** showed H-bonding interactions with Arg87, Ala145, and Gln184 at P1 site of 2QL9. Adjacent to it forms

hydrophobic contacts with Tyr230 and Trp232 at the P2 site; H bonding interaction with Arg233 at P3 site. The P4 pocket of caspase-7 is well suited for hydrophobic contacts with Trp240 and Gln276 residues.

Compound **6n** formed H-bonding interactions with Arg179, Gln283, Cys285 and Ser339 at the P1-P2 site of 1F9E. Additionally, it forms ionic contacts with Arg179 at the P3 site; hydrophobic interaction with Pro343 and Asp381B residues of caspase-8 protein.

As shown in the Figs. 2, 4, 5 and 6 binding site of caspases consist of four hypothetical pockets. A P1 pocket of caspase-1, 3, 7 and 8 enzymes comprised of Arg179, His237, Cys285 and Arg341 residues which mainly exhibit electrostatic and H-bonding interactions. The P2-P3 pockets are highly conserved by Ser339 and Arg341 residues, which involve in H-bonding interactions. The significant difference has been observed in the P4 pocket among the four caspases. The P4 pocket of caspase-1 contains hydrophobic residues such as Trp340, His342 and Val348. However, P4 pockets of Caspase-3, 7 and 8 are comparatively smaller and more hydrophilic compared to Caspase-1. Furthermore, molecular docking studies showed that compounds reside more accurately in the binding site of caspase-1 compared to caspase-3, 7 and 8 proteins. These different binding modes indicated 2,4-diaminopyrimidines having higher specificity for caspase-1 compared to any other caspases.

#### 2.5. Molecular dynamic simulations

After exhibiting significant docking interaction, the protein-ligand complex was subjected to MD simulation [21]. The stability

**Table 1**  
Caspase-1 inhibitory activity of 2,4-diaminopyrimidine derivatives.

Sample code	R	R <sub>1</sub>	IC <sub>50</sub> ± SD (μM)
<b>6a</b>	-H	-H	12.48 ± 0.08
<b>6b</b>	-H	4-CH <sub>3</sub>	4.83 ± 0.05
<b>6c</b>	-H	3-CH <sub>3</sub>	4.51 ± 0.14
<b>6d</b>	-H	4-F	1.86 ± 0.77
<b>6e</b>	4-CH <sub>3</sub>	-H	8.25 ± 0.06
<b>6f</b>	4-OCH <sub>3</sub>	-H	8.73 ± 0.15
<b>6g</b>	4-CH <sub>3</sub>	2-CH <sub>3</sub>	3.78 ± 0.21
<b>6h</b>	4-OCH <sub>3</sub>	3-CH <sub>3</sub>	3.56 ± 0.77
<b>6i</b>	4-CH <sub>3</sub>	4-CH <sub>3</sub>	6.85 ± 0.08
<b>6j</b>	4-CH <sub>3</sub>	4-Cl	1.65 ± 0.16
<b>6k</b>	4-OCH <sub>3</sub>	4-F	1.72 ± 0.12
<b>6l</b>	4-OCH <sub>3</sub>	3-Cl, 4-CH <sub>3</sub>	2.80 ± 0.20
<b>6m</b>	4-F	-H	0.035 ± 0.007
<b>6n</b>	2-F	-H	0.027 ± 0.005
<b>6o</b>	3-Cl	-H	0.022 ± 0.013
<b>6p</b>	4-F	4-CH <sub>3</sub>	0.078 ± 0.015
<b>6q</b>	4-Cl	3-CH <sub>3</sub>	0.052 ± 0.008
<b>6r</b>	4-Cl	2-CH <sub>3</sub>	0.045 ± 0.010
<b>6s</b>	4-F	4-Br	1.75 ± 0.21
<b>6t</b>	2-F	3-CH <sub>3</sub>	0.95 ± 0.13
<b>6u</b>	2,3-di-CH <sub>3</sub>	3,5-di-CH <sub>3</sub>	10.57 ± 0.19
<b>6v</b>	2,3-di-CH <sub>3</sub>	-H	10.81 ± 0.54
<b>6w</b>	2,3-di-CH <sub>3</sub>	4-F	9.78 ± 0.30
Ac-YVAD-CHO	-	-	0.002 ± 0.010

IC<sub>50</sub> values are the mean of triplicate assay.

**Table 2**  
Cell based potential of compounds 6m, 6n, 6o, 6p, 6q and 6r.

Compd.	THP-1 IC <sub>50</sub> ± SD (μM) <sup>a</sup>
<b>6m</b>	6.25 ± 0.06
<b>6n</b>	3.55 ± 0.02
<b>6o</b>	3.20 ± 0.15
<b>6p</b>	8.00 ± 0.30
<b>6q</b>	6.84 ± 0.16
<b>6r</b>	6.37 ± 0.21
<b>Ac-YVAD-CHO</b>	3.95 ± 0.07
<b>MG-132</b>	3.00 ± 0.09

<sup>a</sup> IC<sub>50</sub> the half maximal inhibitory concentration.

of stimulated system was analysed by the RMSD and RMSF values with respect to unbound protein structure. The temporal RMSD plot of caspase-1 and **6p** complex is shown in Fig. 7(a). The curve

exhibited variation in protein backbone and ligand atoms between the 5–10 ns. Further, the RMSF plot of complex revealed that most of residues fluctuate below 2.0 Å and fewer residues showed fluctuation up to 4.5 Å (Fig. 7(b)). High fluctuations were observed in N- and C-terminal region compared to any other part of protein. Subsequently, favourable contacts between the protein residues and ligand atoms were found with Arg341, His237, Gly238, Ser339, Met345, Val348 and Arg383 conserved for more than 25% of MD simulation. Fig. 8 displayed the schematic diagram of protein- ligand interactions. The H-bonding interactions were formed with Arg179, Glu283 and Ser347 which contributed to the binding affinity of ligand. The Arg341 formed pi-cation interaction for about 45% of simulation time. Further, Trp340 and His342 formed pi interaction for more than 33% of simulation period. These essential residues interactions with **6p** supported its inhibitory potency as a potent caspase-1 inhibitor.

## 2.6. In silico prediction of pharmacokinetic (ADME) properties

The computational assessment of ADME (absorption, distribution, metabolism, and excretion) properties was performed using *QikProp* and compared with the reported caspase-1 inhibitors [22]. The theoretical values of ADME parameters, including octanol/water partition coefficient (QPlogPo/w) (−2.0/6.5), aqueous solubility in mol/dm<sup>3</sup> (QPlogS) (−6.5/0.5), apparent Caco-2 cell permeability in nm/s (QPcaco) (>500), pIC<sub>50</sub> for blockade of hERG K<sup>+</sup> channels (QPlogHERG) (<−5) and % human oral absorption (>80) are presented in Table 3. All the compounds (**6a–6w**) displayed QPlogPo/w and QPlogS values in the preferred range of known drugs. Moreover, the calculated QPcaco and % human oral absorption values indicated their good cellular permeability and oral bioavailability. Finally, the compounds were also evaluated for their hERG channel blockade potential.

## 3. Conclusion

A novel series of 2,4-diaminopyrimidine was designed, synthesized and biologically evaluated for their caspase-1 inhibition. Among them six compound **6m**, **6n**, **6o**, **6p**, **6q** and **6r** exhibited good inhibitory activities with IC<sub>50</sub> 0.035, 0.027, 0.022, 0.078, 0.052, and 0.045 μM respectively. The preliminary SAR indicated that accommodation of halogen atom at *ortho* and *meta* position of R ring demonstrated good potency. Further alkyl substitution at the *ortho* and *meta* position of R<sub>1</sub> ring exhibited remarkable shift in the activity, leading to micromolar potency. In short, sizes and electronic properties of the substituents may explain the structural requirements for potent caspase-1 inhibition. As caspase-1 is

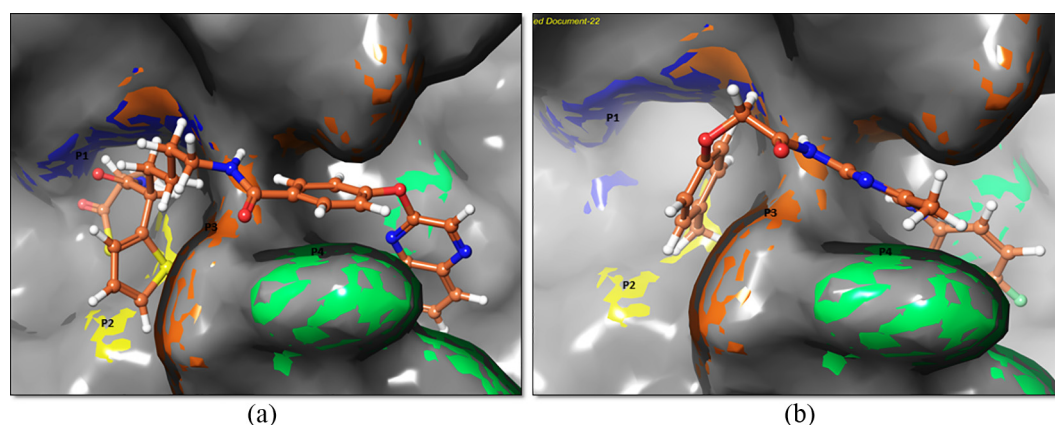


**Fig. 2.** (a) Binding mode of Co-crystal ligand in the binding site of caspase-1 (1RWX) (b) Binding mode of **6p** in the binding site of caspase-1 (1RWX).

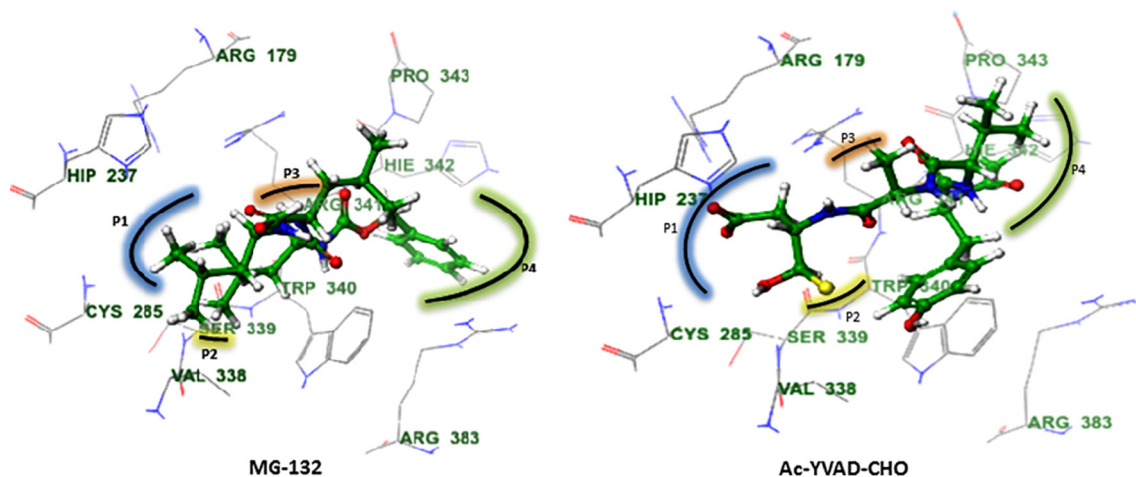


Fig. 3. (a) Binding pose of MG-132 in the active site of caspase-1 (1RWX) (b) Binding pose of Ac-YVAD-CHO in the active site of caspase-1 (1RWX).

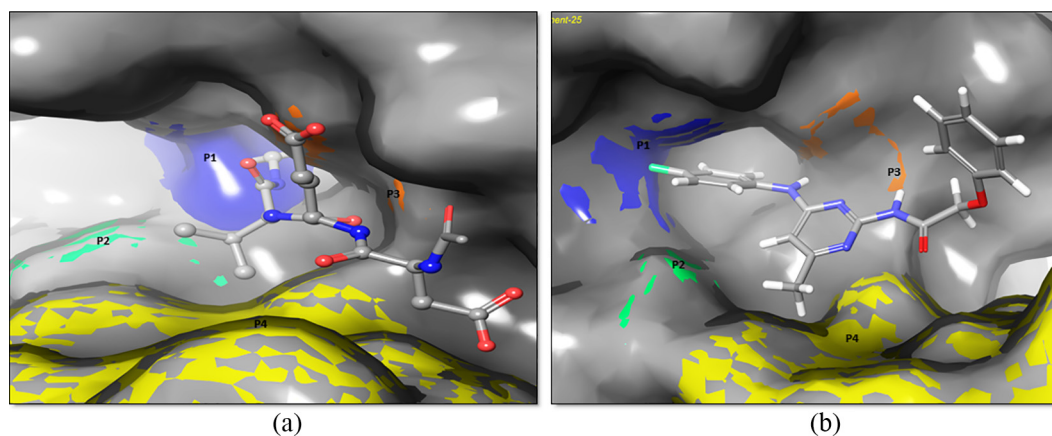


Fig. 4. (a) Binding mode of Co-crystal ligand in the binding site of caspase-3 (1PAU) (b) Binding mode of 6 m in the binding site of caspase-3 (1PAU).

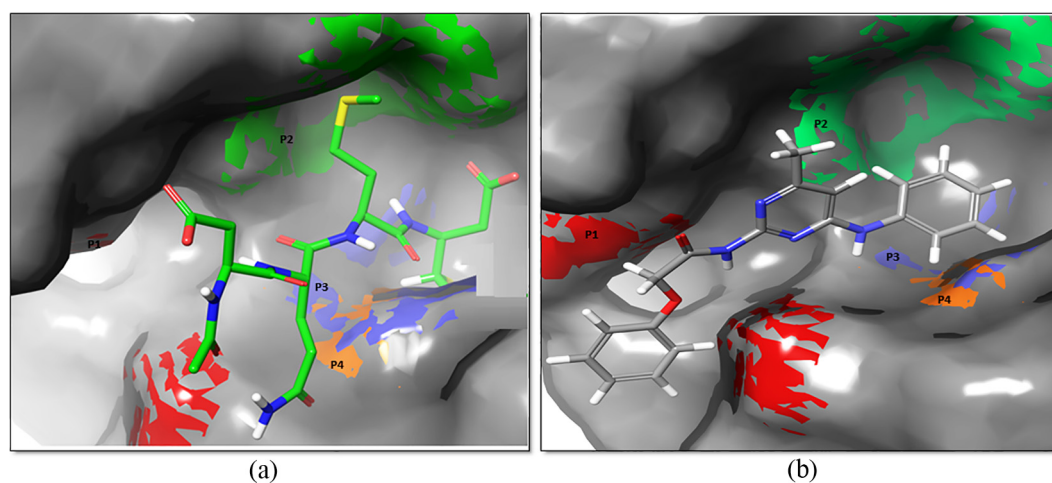
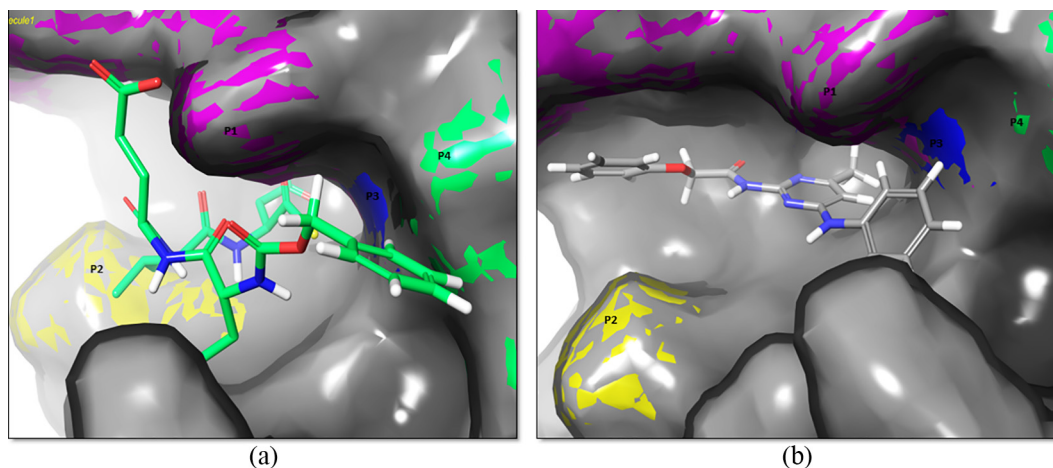


Fig. 5. (a) Binding mode of Co-crystal ligand in the binding site of caspase-7 (2QL9) (b) Binding mode of 6a in the binding site of caspase-7 (2QL9).

endogenous protease the potent compounds were also evaluated for their cell based activity. Compound **6m**, **6n**, **6o**, **6p**, **6q** and **6r** displayed the modest cell based potency with  $IC_{50}$  6.25, 3.55, 3.20, 8.0, 6.84 and 6.37  $\mu$ M respectively. Further, the molecular

docking studies explain the selectivity and provide important insight for designing newer series of compounds. These results demonstrated that compound **6m**, **6n** and **6o** might be promising leads for their further development as novel caspase-1 inhibitors.



**Fig. 6.** (a) Binding mode of Co-crystal ligand in the binding site of caspase-8 (1F9E) (b) Binding mode of 6n in the binding site of caspase-8 (1F9E) (Blue: Polar interaction; Yellow: H-Bond interaction; Green colour: Hydrophobic interaction; Orange, red & pink colour: ionic interaction). (For interpretation of the references to colour in this figure legend, the reader is referred to the web version of this article.)

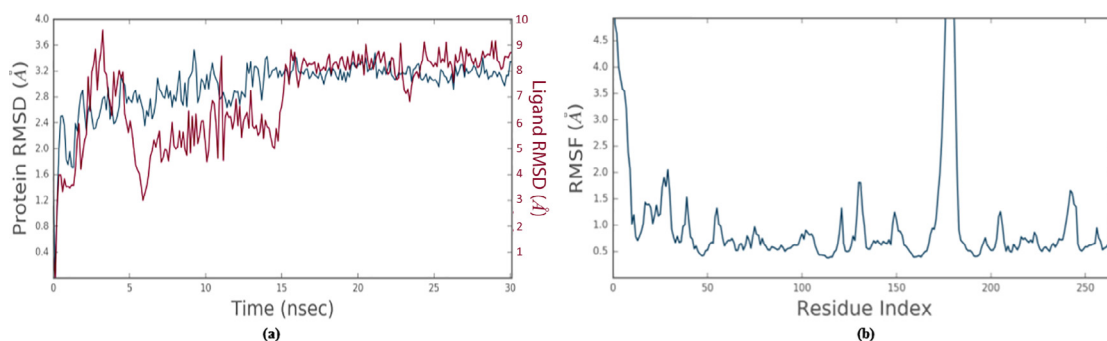


**Fig. 7.** (a) RMSD plot of caspase-1-6p complex (b) RMSF plot of flexible region of Caspase-1 Protein.

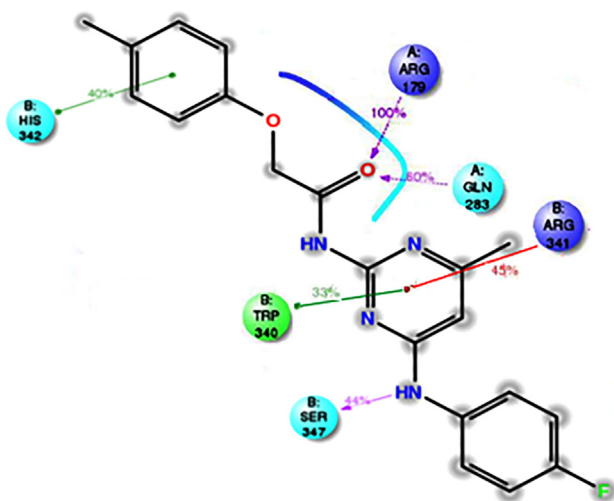


**Fig. 8.** Protein –Ligand Interactions.

## 4. Experimental section

### 4.1. Chemistry

All the chemical reagents were purchased from commercially available sources and used without further purification. The solvents were distilled and dried according to standard procedures.

Melting points of all synthesized compounds were determined in open capillaries, microprocessor based melting point apparatus VMP-D (VEEGO) and reported uncorrected. TLC was performed on silica gel pre-coated aluminium plates (Merck60 F254, 0.25 mm) and spots were visualized by iodine vapours and UV irradiation. The IR spectra of the final compounds were recorded in KBr using Shimadzu FT-IR 8400S.  $^1\text{H}$  NMR and  $^{13}\text{C}$  NMR spectra were measured on Bruker AVANCE-II 400 MHz spectrophotometer using TMS as an internal standard and  $\text{DMSO-}d_6$  as solvent. Chemical shifts were given in  $\delta$  ppm and coupling constant ( $J$ ) in Hz; splitting patterns were described as s (singlet), d (doublet), t (triplet), q (quartet) or m (multiplet). The mass spectra were taken using SHIMADZU LCMS 2010 EV. Synthesis of *N*-(4-((substituted phenyl)amino)-6-methylpyrimidin-2-yl)-2-substituted phenoxy acetamide derivatives were performed by following experimental protocol, characterized by above discussed physical and spectroscopic techniques.

#### 4.1.1. 2-Amino-4-hydroxy-6-methylpyrimidin (3)

Guanidine hydrochloride (0.17gm, 0.0018 mol) was neutralised using NaOH (0.08gm, 0.0022 mol) in ethanol. Ethyl acetoacetate (0.2 ml, 0.0018 mol) was added drop wise and reaction mixture was stirred for 3–4 h at room temperature. Cyclocondensation of guanidine with ethyl acetoacetate [14] gave white solid which was filtered, washed with water, dried and recrystallized using ethanol.

#### 4.1.2. 2-Amino-4-chloro-6-methylpyrimidin (4)

To a solution of compound 3 (0.16gm, 0.0013 mol) in toluene, phosphorous oxychloride (0.9 ml, 0.0104 mol) [15] was added

**Table 3**  
ADMET properties of synthesized compounds (6a–6w).

Compound	QPlogPo/w	QPlogS	QPPCaco	QPlogHERG	% Human Oral Absorption
<b>6a</b>	3.643	−5.471	1006.137	−7.262	100
<b>6b</b>	3.945	−6.023	1004.585	−7.144	100
<b>6c</b>	3.944	−6.026	1006.674	−7.147	100
<b>6d</b>	3.876	−5.833	1004.773	−7.130	100
<b>6e</b>	3.947	−5.772	1412.142	−6.939	100
<b>6f</b>	3.530	−5.687	1004.463	−7.114	100
<b>6g</b>	4.265	−6.517	1092.106	−7.032	100
<b>6h</b>	3.315	−6.241	1004.673	−6.995	100
<b>6i</b>	4.248	−6.588	1006.151	−7.025	100
<b>6j</b>	4.433	−6.352	1003.643	−7.028	100
<b>6k</b>	3.539	−6.054	1004.169	−6.986	100
<b>6l</b>	3.643	−6.531	1006.137	−7.262	100
<b>6m</b>	3.866	−5.584	1361.929	−6.924	100
<b>6n</b>	3.876	−5.779	1078.471	−7.138	100
<b>6o</b>	4.130	−6.191	1005.099	−7.148	100
<b>6p</b>	4.167	−6.136	1364.412	−6.812	100
<b>6q</b>	4.433	−6.205	1005.631	−7.028	100
<b>6r</b>	4.130	−6.193	1004.219	−7.149	100
<b>6s</b>	4.430	−6.435	1358.565	−6.856	100
<b>6t</b>	4.178	−6.335	1078.756	−7.021	100
<b>6u</b>	4.849	−6.546	1116.825	−6.822	100
<b>6v</b>	4.261	−6.583	1196.565	−7.039	100
<b>6w</b>	4.493	−6.550	1183.331	−6.907	100
<b>VX-740</b>	0.759	−3.647	84.463	−4.597	39.956
<b>VX-765</b>	1.255	−4.029	181.383	−2.563	61.763

and heated at 110 °C for 30 min. The excess POCl<sub>3</sub> was distilled off and gummy residue was poured in to ice cold water. Neutralization with NaHCO<sub>3</sub> gave yellow solid which was recrystallized from methanol.

#### 4.1.3. General procedure for synthesis of 2-amino-4-(4-substituted phenylamino)-6-methylpyrimidin (**5a–5j**)

To a suspension of compound **4** (0.50gm, 0.0035 mol) in 20 ml ethanol, substituted aniline (0.0035 mol) and 2–5 drops of conc. HCl was added [16,17]. The reaction mixture was refluxed till the completion of reaction indicated by TLC. Then crude solid was filtered, dried and recrystallized by methanol to obtain the title compounds **5a–5j**.

#### 4.1.4. General procedure for synthesis of 2-(substituted phenoxy) acetyl chloride

Substituted phenol (0.05 mol) was dissolved in the aqueous solution of NaOH (0.60gm, 0.015 mol), chloroacetic acid (0.70gm, 0.0075 mol) was added and reaction mixture was refluxed for 3 h [23,24]. After completion of the reaction, mixture was acidified with conc. HCl, precipitated solid was filtered, dried and recrystallized from hot water. The resultant compound (0.003 mol) was dissolved in toluene, SOCl<sub>2</sub> (0.32 ml, 0.0045 mol) was added and refluxed for 1 h. Excess of thionyl chloride was distilled off and viscous residue was immediately used for further reaction.

#### 4.1.5. General procedure for synthesis of N-(4-(substituted phenyl) amino)-6-methylpyrimidin-2-yl)-2-substituted phenoxy acetamide (**6a–6w**)

To a solution of 2-amino-4-(4-substituted phenylamino)-6-methylpyrimidin (0.003 mol) in 10 ml of DMF, TEA (0.0033 mol) was added and stirred for 15 min. 2-(substituted phenoxy) acetyl chloride (0.003 mol) was added drop wise and reaction mixture was stirred at 5 °C for 1 h. After completion of reaction, mixture was poured into ice cold water. The obtained solid was recrystallized using ethyl acetate to yield pure product.

**4.1.5.1. N-(4-methyl-6-(phenylamino)pyrimidin-2-yl)-2-phenoxyacetamide (6a).** White solid; yield: 43.34%; M.P.: 202–204 °C; IR

(KBr)  $\nu$  (cm<sup>−1</sup>): 3244, 3190, 2995, 1681, 1070; <sup>1</sup>H NMR (400 MHz, DMSO *d*<sub>6</sub>):  $\delta$ 10.30 (s, 1H, CONH), 9.49 (s, 1H, NH), 7.84 (d, *J* = 8.0 Hz, 2H, Ar–H), 7.28 (t, *J* = 4.4 Hz, 4H, Ar–H), 6.98 (t, *J* = 7.2 Hz, 2H, Ar–H), 6.92 (d, *J* = 7.6 Hz, 2H, Ar–H), 6.35 (s, 1H, Ar–H), 4.93 (s, 2H, OCH<sub>2</sub>), 2.25 (s, 3H, CH<sub>3</sub>); <sup>13</sup>C NMR (400 MHz, DMSO *d*<sub>6</sub>):  $\delta$ 167.45, 165.20, 160.99, 157.90, 156.44, 139.89, 129.43, 128.65, 122.08, 120.83, 119.78, 114.40, 100.37, 67.31, 23.37; LC-MS: *m/z* calculated for C<sub>19</sub>H<sub>18</sub>N<sub>4</sub>O<sub>2</sub>: 334.4; found: 335.5 [M+1]<sup>+</sup>.

**4.1.5.2. N-(4-methyl-6-(phenylamino)pyrimidin-2-yl)-2-(*p*-tolylloxy)acetamide (6b).** White solid; yield: 48.46%; M.P.: 230–232 °C; IR (KBr)  $\nu$  (cm<sup>−1</sup>): 3344, 3172, 2989, 1668, 1070; <sup>1</sup>H NMR (400 MHz, DMSO *d*<sub>6</sub>):  $\delta$ 12.08 (s, 1H, CONH), 11.63 (s, 1H, NH), 7.88 (d, *J* = 8.0 Hz, 2H, Ar–H), 7.41 (t, *J* = 4.2 Hz, 2H, Ar–H), 7.20 (t, *J* = 7.6 Hz, 3H, Ar–H), 6.89 (d, *J* = 8.0 Hz, 3H, Ar–H), 6.798 (s, 1H, Ar–H) 4.95 (s, 2H, OCH<sub>2</sub>), 2.50 (s, 3H, CH<sub>3</sub>), 2.23 (s, 3H, CH<sub>3</sub>); <sup>13</sup>C NMR (400 MHz, DMSO *d*<sub>6</sub>):  $\delta$ 170.02, 160.99, 155.43, 151.36, 137.68, 130.04, 129.80, 128.89, 124.87, 121.59, 114.40, 102.20, 66.60, 20.45, 19.40; LC-MS: *m/z* calculated for C<sub>20</sub>H<sub>20</sub>N<sub>4</sub>O<sub>2</sub>: 348.4; found: 349.4 [M+1]<sup>+</sup>.

**4.1.5.3. N-(4-methyl-6-(phenylamino)pyrimidin-2-yl)-2-(*m*-tolylloxy)acetamide (6c).** White solid; yield: 46.4%; M.P.: 160–162 °C; IR (KBr)  $\nu$  (cm<sup>−1</sup>): 3249, 3188, 2987, 1681, 1080; <sup>1</sup>H NMR (400 MHz, DMSO *d*<sub>6</sub>):  $\delta$ 10.32 (s, 1H, CONH),  $\delta$ 9.52 (s, 1H, NH), 7.85 (d, *J* = 6.0 Hz, 2H, Ar–H), 7.29 (t, *J* = 4.4 Hz, 2H, Ar–H), 7.157 (t, *J* = 4.0 Hz, 1H, Ar–H), 6.99 (s, 1H, Ar–H), 6.773 (t, *J* = 8.8 Hz, 1H, Ar–H), 6.699 (d, *J* = 8.0 Hz, 2H, Ar–H), 6.34 (s, 1H, Ar–H), 4.90 (s, 2H, OCH<sub>2</sub>), 2.26 (s, 6H, CH<sub>3</sub>); <sup>13</sup>C NMR (400 MHz, DMSO *d*<sub>6</sub>):  $\delta$ 167.47, 165.19, 160.99, 157.92, 156.44, 139.91, 138.89, 129.15, 128.64, 122.05, 121.60, 119.74, 115.11, 111.34, 100.38, 67.27, 23.36, 21.09; LC-MS: *m/z* calculated for C<sub>20</sub>H<sub>20</sub>N<sub>4</sub>O<sub>2</sub>: 348.4; found: 349.4 [M+1]<sup>+</sup>.

**4.1.5.4. 2-(4-Fluorophenoxy)-N-(4-methyl-6-(phenylamino)pyrimidin-2-yl)acetamide (6d).** White solid; yield: 34.09%; M.P.: 205–207 °C; IR (KBr)  $\nu$  (cm<sup>−1</sup>): 3238, 3155, 2989, 1685, 1066; <sup>1</sup>H NMR (400 MHz, DMSO *d*<sub>6</sub>):  $\delta$ 10.35 (s, 1H, CONH), 9.52 (s, 1H, NH),  $\delta$ 7.84 (d, *J* = 8.0 Hz, 2H, Ar–H), 7.28 (t, *J* = 7.6 Hz, 2H, Ar–H), 7.09

(t,  $J = 8.8$  Hz, 2H, Ar-H), 6.96 (t,  $J = 7.6$  Hz, 1H, Ar-H), 6.92 (d,  $J = 4.4$  Hz, 2H, Ar-H), 6.35 (s, 1H, Ar-H), 4.93 (s, 2H, OCH<sub>2</sub>), 2.25 (s, 3H, CH<sub>3</sub>); <sup>13</sup>C NMR (400 MHz, DMSO *d*<sub>6</sub>):  $\delta$ 167.30, 165.20, 160.99, 156.84, 151.36, 139.85, 129.15, 122.12, 119.84, 116.21, 100.34, 67.64, 23.37; LCMS: *m/z* calculated for C<sub>19</sub>H<sub>17</sub>FN<sub>4</sub>O<sub>2</sub>: 352.4; found: 353.4 [M+1]<sup>+</sup>.

4.1.5.5. *N*-(4-methyl-6-(*p*-tolylamino)pyrimidin-2-yl)-2-phenoxyacetamide (**6e**). White solid; yield: 46.26%; M.P.: 205–206 °C; IR (KBr)  $\nu$  (cm<sup>-1</sup>): 3363, 3301, 3035, 1681, 1066; <sup>1</sup>H NMR (400 MHz, DMSO *d*<sub>6</sub>):  $\delta$ 10.27 (s, 1H, CONH), 9.40 (s, 1H, NH), 7.67 (d,  $J = 8.0$  Hz, 2H, Ar-H), 7.28 (t,  $J = 8.0$  Hz, 2H, Ar-H), 7.07 (d,  $J = 8.0$  Hz, 2H, Ar-H), 6.94 (t,  $J = 7.2$  Hz, 1H, Ar-H), 6.89 (d,  $J = 8.0$  Hz, 2H, Ar-H), 6.29 (s, 1H, Ar-H), 4.93 (s, 2H, OCH<sub>2</sub>), 2.23 (s, 6H, CH<sub>3</sub>); <sup>13</sup>C NMR (400 MHz, DMSO *d*<sub>6</sub>):  $\delta$ 167.54, 165.05, 161.05, 157.92, 156.49, 137.23, 131.11, 129.41, 129.10, 120.80, 120.10, 114.41, 100.01, 67.37, 23.35, 20.38; LC-MS: *m/z* calculated for C<sub>20</sub>H<sub>20</sub>N<sub>4</sub>O<sub>2</sub>: 348.4; found: 349.4 [M+1]<sup>+</sup>.

4.1.5.6. *N*-(4-((4-methoxyphenyl)amino)-6-methylpyrimidin-2-yl)-2-phenoxyacetamide (**6f**). White solid; yield: 56.22%; M.P.: 175–177 °C; IR (KBr)  $\nu$  (cm<sup>-1</sup>): 3242, 3218, 2937, 1679, 1062; <sup>1</sup>H NMR (400 MHz, DMSO *d*<sub>6</sub>):  $\delta$ 10.28 (s, 1H, CONH), 9.35 (s, 1H, NH), 7.69 (d,  $J = 8.0$  Hz, 2H, Ar-H), 7.26 (t,  $J = 7.6$  Hz, 2H, Ar-H), 6.945 (t,  $J = 7.6$  Hz, 1H, Ar-H), 6.88 (d,  $J = 8.8$  Hz, 4H, Ar-H), 6.24 (s, 1H, Ar-H), 4.92 (s, 2H, OCH<sub>2</sub>), 3.70 (s, 3H, OCH<sub>3</sub>), 2.22 (s, 3H, CH<sub>3</sub>); <sup>13</sup>C NMR (400 MHz, DMSO *d*<sub>6</sub>):  $\delta$ 167.59, 164.91, 161.09, 157.88, 156.49, 154.77, 132.75, 129.39, 121.82, 120.77, 114.36, 113.84, 100.09, 67.34, 55.05, 23.32; LC-MS: *m/z* calculated for C<sub>20</sub>H<sub>20</sub>N<sub>4</sub>O<sub>3</sub>: 364.4; found: 365.2 [M+1]<sup>+</sup>.

4.1.5.7. *N*-(4-methyl-6-(*p*-tolylamino)pyrimidin-2-yl)-2-(*o*-tolylloxy)acetamide (**6g**). White solid; yield: 39.56%; M.P.: 196–199 °C; IR (KBr)  $\nu$  (cm<sup>-1</sup>): 3242, 2937, 1679, 1600, 1492, 1280, 1247, 1031, 823; <sup>1</sup>H NMR (400 MHz, DMSO *d*<sub>6</sub>):  $\delta$ 10.24 (s, 1H, CONH), 9.41 (s, 1H, NH), 7.68 (d,  $J = 8.0$  Hz, 2H, Ar-H), 7.12 (t,  $J = 7.2$  Hz, 1H, Ar-H), 7.09 (d,  $J = 8.0$  Hz, 2H, Ar-H), 6.84 (t,  $J = 7.6$  Hz, 1H, Ar-H), 6.75 (d,  $J = 8.4$  Hz, 1H, Ar-H), 6.30 (s, 1H, Ar-H), 4.96 (s, 2H, OCH<sub>2</sub>), 2.50 (s, 6H, CH<sub>3</sub>), 1.99 (s, 3H, CH<sub>3</sub>); <sup>13</sup>C NMR (400 MHz, DMSO *d*<sub>6</sub>):  $\delta$ 167.54, 165.05, 161.05, 157.92, 156.49, 137.23, 131.11, 129.41, 126.60, 120.10, 114.41, 100.01, 67.37, 23.35, 20.38, 20.02; LC-MS: *m/z* calculated for C<sub>21</sub>H<sub>22</sub>N<sub>4</sub>O<sub>2</sub>: 362.4; found: 363.5 [M+1]<sup>+</sup>.

4.1.5.8. *N*-(4-((4-methoxyphenyl)amino)-6-methylpyrimidin-2-yl)-2-(*m*-tolylloxy)acetamide (**6h**). White solid; yield: 44.43%; M.P.: 162–164 °C; IR (KBr)  $\nu$  (cm<sup>-1</sup>): 3245, 3093, 2958, 1681, 1074; <sup>1</sup>H NMR (400 MHz, DMSO *d*<sub>6</sub>):  $\delta$ 10.24 (s, 1H, CONH), 9.35 (s, 1H, NH), 7.69 (d,  $J = 6.4$  Hz, 2H, Ar-H), 7.16 (t,  $J = 7.6$  Hz, 1H, Ar-H), 6.86 (d,  $J = 8.4$  Hz, 2H, Ar-H), 6.76 (d,  $J = 7.2$  Hz, 1H, Ar-H), 6.67 (d,  $J = 8.8$  Hz, 1H, Ar-H), 6.24 (s, 2H, Ar-H), 4.90 (s, 2H, OCH<sub>2</sub>), 3.70 (s, 3H, OCH<sub>3</sub>), 2.26 (s, 6H, CH<sub>3</sub>); <sup>13</sup>C NMR (400 MHz, DMSO *d*<sub>6</sub>):  $\delta$ 167.63, 164.91, 161.09, 157.92, 156.51, 154.74, 138.87, 132.80, 129.14, 121.79, 121.57, 115.10, 113.85, 111.31, 99.69, 67.31, 55.06, 23.33, 21.07; LC-MS: *m/z* calculated for C<sub>21</sub>H<sub>22</sub>N<sub>4</sub>O<sub>3</sub>: 378.4; found: 379.3 [M+1]<sup>+</sup>.

4.1.5.9. *N*-(4-Methyl-6-(*p*-tolylamino)pyrimidin-2-yl)-2-(*p*-tolylloxy)acetamide (**6i**). Orange solid; yield: 44.07%; M.P.: 205–206 °C; IR (KBr)  $\nu$  (cm<sup>-1</sup>): 3330, 3220, 2943, 1687, 1070; <sup>1</sup>H NMR (400 MHz, DMSO *d*<sub>6</sub>):  $\delta$ 10.20 (s, 1H, CONH), 9.39 (s, 1H, NH), 7.68 (d,  $J = 7.6$  Hz, 2H, Ar-H), 7.082 (d,  $J = 4.0$  Hz, 4H, Ar-H), 6.79 (d,  $J = 8.0$  Hz, 2H, Ar-H), 6.30 (s, 1H, Ar-H), 4.88 (s, 2H, OCH<sub>2</sub>), 2.22 (s, 9H, CH<sub>3</sub>); <sup>13</sup>C NMR (400 MHz, DMSO *d*<sub>6</sub>):  $\delta$ 167.64, 165.03, 161.07, 156.50, 155.83, 137.25, 131.09, 129.72, 129.48, 129.09, 120.10, 114.25, 100.07, 67.55, 23.33, 20.37, 20.02; LC-MS: *m/z* calculated for C<sub>21</sub>H<sub>22</sub>N<sub>4</sub>O<sub>2</sub>: 362.4; found: 363.5 [M+1]<sup>+</sup>.

4.1.5.10. 2-(4-Chlorophenoxy)-*N*-(4-methyl-6-(*p*-tolylamino)pyrimidin-2-yl)acetamide (**6j**). White solid; yield: 41.65%; M.P.: 191–194 °C; IR (KBr)  $\nu$  (cm<sup>-1</sup>): 3242, 3186, 2989, 1681, 1058; <sup>1</sup>H NMR (400 MHz, DMSO *d*<sub>6</sub>):  $\delta$ 10.29 (s, 1H, CONH), 9.38 (s, 1H, NH), 7.65 (d,  $J = 8$  Hz, 2H, Ar-H), 7.32 (d,  $J = 8.8$  Hz, 2H, Ar-H), 7.09 (d,  $J = 8.4$  Hz, 2H, Ar-H), 6.92 (d,  $J = 8.8$  Hz, 2H, Ar-H), 6.29 (s, 1H, Ar-H), 4.96 (s, 2H, OCH<sub>2</sub>), 2.23 (s, 6H, CH<sub>3</sub>); <sup>13</sup>C NMR (400 MHz, DMSO *d*<sub>6</sub>):  $\delta$ 167.43, 165.05, 161.06, 156.85, 156.48, 137.18, 131.18, 129.12, 129.10, 124.46, 120.19, 116.21, 99.99, 67.72, 23.35, 20.37; LC-MS: *m/z* calculated for C<sub>20</sub>H<sub>19</sub>ClN<sub>4</sub>O<sub>2</sub>: 382.8; found: 383.4 [M+1]<sup>+</sup>, 385.4 [M+2]<sup>+</sup>.

4.1.5.11. 2-(4-fluorophenoxy)-*N*-(4-((4-methoxyphenyl)amino)-6-methylpyrimidin-2-yl)acetamide (**6k**). White solid; yield: 55.25%; M.P.: 192–194 °C; IR (KBr)  $\nu$  (cm<sup>-1</sup>): 3236, 3155, 2977, 1681, 1062; <sup>1</sup>H NMR (400 MHz, DMSO *d*<sub>6</sub>):  $\delta$ 10.25 (s, 1H, CONH), 9.33 (s, 1H, NH), 7.67 (d,  $J = 8$  Hz, 2H, Ar-H), 7.13 (d,  $J = 8.8$  Hz, 2H, Ar-H), 6.90 (d,  $J = 4.4$  Hz, 4H, Ar-H), 6.24 (s, 1H, Ar-H), 4.91 (s, 2H, OCH<sub>2</sub>), 3.70 (s, 3H, OCH<sub>3</sub>), 2.22 (s, 3H, CH<sub>3</sub>); <sup>13</sup>C NMR (400 MHz, DMSO *d*<sub>6</sub>):  $\delta$ 167.57, 164.94, 161.13, 157.76, 156.61, 155.41, 154.83, 154.28, 132.74, 121.95, 115.84, 115.66, 113.87, 99.60, 68.01, 55.07, 23.33; LC-MS: *m/z* calculated for C<sub>20</sub>H<sub>19</sub>FN<sub>4</sub>O<sub>3</sub>: 382.4; found: 383.3 [M+1]<sup>+</sup>.

4.1.5.12. 2-(3-Chloro-4-methylphenoxy)-*N*-(4-((4-methoxyphenyl)amino)-6-methylpyrimidin-2-yl)acetamide (**6l**). White solid; yield: 48.29%; M.P.: 189–190 °C; IR (KBr)  $\nu$  (cm<sup>-1</sup>): 3240, 3122, 2962, 1683, 1037; <sup>1</sup>H NMR (400 MHz, DMSO *d*<sub>6</sub>):  $\delta$ 10.25 (s, 1H, CONH), 9.34 (s, 1H, NH), 7.66 (d,  $J = 7.2$  Hz, 2H, Ar-H), 7.29 (s, 1H, Ar-H), 6.91 (d,  $J = 2.8$  Hz, 1H, Ar-H), 6.86 (d,  $J = 8.8$  Hz, 2H, Ar-H), 6.73 (d,  $J = 2.8$  Hz, 1H, Ar-H), 6.24 (s, 1H, Ar-H), 4.93 (s, 2H, OCH<sub>2</sub>), 3.69 (s, 3H, OCH<sub>3</sub>), 2.27 (s, 3H, CH<sub>3</sub>), 2.22 (s, 3H, CH<sub>3</sub>); <sup>13</sup>C NMR (400 MHz, DMSO *d*<sub>6</sub>):  $\delta$ 167.52, 164.94, 161.11, 156.74, 156.51, 154.80, 136.34, 132.73, 129.37, 124.77, 121.91, 117.28, 113.45, 100, 67.63, 55.06, 23.34, 19.76; LC-MS: *m/z* calculated for C<sub>21</sub>H<sub>21</sub>-ClN<sub>4</sub>O<sub>3</sub>: 412.9; found: 413.2 [M+1]<sup>+</sup>, 415.3 [M+2]<sup>+</sup>.

4.1.5.13. *N*-(4-((4-fluorophenyl)amino)-6-methylpyrimidin-2-yl)-2-phenoxyacetamide (**6m**). White solid; yield: 40.95%; M.P.: 178–180 °C; IR (KBr)  $\nu$  (cm<sup>-1</sup>): 3249, 3128, 2993, 1681, 1066; <sup>1</sup>H NMR (400 MHz, DMSO *d*<sub>6</sub>):  $\delta$ 10.36 (s, 1H, CONH), 9.55 (s, 1H, NH), 7.89 (d,  $J = 4.8$  Hz, 2H, Ar-H), 7.87 (d,  $J = 7.2$  Hz, 2H, Ar-H), 7.29 (t,  $J = 6.8$  Hz, 2H, Ar-H), 7.12 (t,  $J = 7.2$  Hz, 1H, Ar-H), 6.97 (d,  $J = 8.0$  Hz, 2H, Ar-H), 6.30 (s, 1H, Ar-H), 4.98 (s, 2H, OCH<sub>2</sub>),  $\delta$  2.25 (s, 3H, CH<sub>3</sub>); <sup>13</sup>C NMR (400 MHz, DMSO *d*<sub>6</sub>):  $\delta$ 167.53, 165.20, 160.85, 158.64, 156.38, 156.27, 138.31, 129.54, 121.40, 117.97, 114.97, 100.22, 67.45, 23.31; LC-MS: *m/z* calculated for C<sub>19</sub>H<sub>17</sub>FN<sub>4</sub>O<sub>2</sub>: 352.4; found: 353.5 [M+1]<sup>+</sup>.

4.1.5.14. *N*-(4-((2-fluorophenyl)amino)-6-methylpyrimidin-2-yl)-2-phenoxyacetamide (**6n**). White solid; yield: 34.76%; M.P.: 183–186 °C; IR (KBr)  $\nu$  (cm<sup>-1</sup>): 3234, 3126, 2991, 1677, 1070; <sup>1</sup>H NMR (400 MHz, DMSO-*d*<sub>6</sub>):  $\delta$ 10.29 (s, 1H, CONH), 9.24 (s, 1H, NH), 8.31 (d,  $J = 8.0$  Hz, 1H, Ar-H), 7.29 (t,  $J = 7.6$  Hz, 1H, Ar-H), 7.15 (d,  $J = 6.4$  Hz, 2H, Ar-H), 7.11 (t,  $J = 3.6$  Hz, 1H, Ar-H), 7.09 (d,  $J = 2.0$  Hz, 1H, Ar-H), 6.95 (t,  $J = 7.2$  Hz, 1H, Ar-H), 6.86 (d,  $J = 8.4$  Hz, 2H, Ar-H), 6.47 (s, 1H, Ar-H), 4.89 (s, 2H, OCH<sub>2</sub>), 2.25 (s, 3H, CH<sub>3</sub>); <sup>13</sup>C NMR (400 MHz, DMSO *d*<sub>6</sub>):  $\delta$ 167.84, 165.72, 161.38, 157.90, 156.39, 155.02, 138.83, 129.11, 127.01, 124.44, 121.53, 115.31, 114.31, 100.32, 67.24, 23.40; LC-MS: *m/z* calculated for C<sub>19</sub>H<sub>17</sub>FN<sub>4</sub>O<sub>2</sub>: 352.4; found: 353.5 [M+1]<sup>+</sup>.

4.1.5.15. *N*-(4-((3-chlorophenyl)amino)-6-methylpyrimidin-2-yl)-2-phenoxyacetamide (**6o**). White solid; yield: 45.29%; M.P.: 172–174 °C; IR (KBr)  $\nu$  (cm<sup>-1</sup>): 3251, 3136, 2935, 1683, 1078; <sup>1</sup>H NMR (400 MHz, DMSO-*d*<sub>6</sub>):  $\delta$ 10.44 (s, 1H, CONH), 9.70 (s, 1H, NH),

8.14 (s, 1H, Ar-H), 7.76 (d,  $J = 1.2$  Hz, 1H, Ar-H), 7.27 (t,  $J = 2.0$  Hz, 3H, Ar-H), 7.01 (t,  $J = 1.2$  Hz, 1H, Ar-H), 6.98 (d,  $J = 6.0$  Hz, 3H, Ar-H), 6.36 (s, 1H, Ar-H), 4.91 (s, 2H, OCH<sub>2</sub>), 2.28 (s, 3H, CH<sub>3</sub>); <sup>13</sup>C NMR (400 MHz, DMSO-*d*<sub>6</sub>): δ167.21, 165.56, 157.88, 156.31, 141.50, 133.25, 130.12, 129.43, 121.46, 120.88, 118.84, 117.73, 114.44, 100.87, 67.32, 23.36; LC-MS:  $m/z$  calculated for C<sub>19</sub>H<sub>17</sub>ClN<sub>4</sub>O<sub>2</sub>: 368.8; found: 369.3 [M+1]<sup>+</sup>, 371.3 [M+2]<sup>+</sup>.

4.1.5.16. *N*-(4-((4-fluorophenyl)amino)-6-methylpyrimidin-2-yl)-2-(*p*-tolylxy)acetamide (**6p**). Orange solid; yield: 39.77%; M.P.: 206–208 °C; IR (KBr)  $\nu$  (cm<sup>-1</sup>): 3330, 3105, 2995, 1691, 1076; <sup>1</sup>H NMR (400 MHz, DMSO-*d*<sub>6</sub>): δ10.28 (s, 1H, CONH), 9.57 (s, 1H, NH), 7.87 (d,  $J = 5.2$  Hz, 2H, Ar-H), 7.12 (d,  $J = 8.8$  Hz, 2H, Ar-H), 7.09 (d,  $J = 2.8$  Hz, 2H, Ar-H), 6.80 (d,  $J = 8.4$  Hz, 2H, Ar-H), 6.31 (s, 1H, Ar-H), 4.87 (s, 2H, OCH<sub>2</sub>), 2.22 (s, 6H, CH<sub>3</sub>); <sup>13</sup>C NMR (400 MHz, DMSO-*d*<sub>6</sub>): δ167.53, 165.20, 160.85, 158.64, 156.27, 155.79, 136.31, 129.73, 129.54, 121.40, 115.19, 114.97, 100.22, 67.45, 23.31; LC-MS:  $m/z$  calculated for C<sub>20</sub>H<sub>19</sub>FN<sub>4</sub>O<sub>2</sub>: 366.4; found: 367.4 [M+1]<sup>+</sup>.

4.1.5.17. *N*-(4-((4-chlorophenyl)amino)-6-methylpyrimidin-2-yl)-2-(*m*-tolylxy)acetamide (**6q**). White solid; yield: 24.03%; M.P.: 180–181 °C; IR (KBr)  $\nu$  (cm<sup>-1</sup>): 3247, 3145, 2987, 1683, 1074; <sup>1</sup>H NMR (400 MHz, DMSO-*d*<sub>6</sub>): δ10.35 (s, 1H, CONH), 9.64 (s, 1H, NH), 7.93 (d,  $J = 8.8$  Hz, 2H, Ar-H), 7.30 (d,  $J = 8.8$  Hz, 2H, Ar-H), 7.18 (t,  $J = 8.0$  Hz, 1H, Ar-H), 6.77 (d,  $J = 7.6$  Hz, 2H, Ar-H), 6.70 (d,  $J = 8.4$  Hz, 1H, Ar-H), 6.34 (s, 1H, Ar-H), 4.89 (s, 2H, OCH<sub>2</sub>), 2.26 (s, 6H, CH<sub>3</sub>); <sup>13</sup>C NMR (400 MHz, DMSO *d*<sub>6</sub>): δ167.41, 165.42, 160.68, 157.89, 156.33, 138.98, 138.91, 129.17, 128.40, 125.40, 121.63, 121.05, 115.10, 111.32, 100.63, 67.20, 23.37, 21.08; LC-MS:  $m/z$  calculated for C<sub>20</sub>H<sub>19</sub>ClN<sub>4</sub>O<sub>2</sub>: 382.8; found: 383.4 [M+1]<sup>+</sup>, 385.4 [M+2]<sup>+</sup>.

4.1.5.18. *N*-(4-((4-chlorophenyl)amino)-6-methylpyrimidin-2-yl)-2-phenoxyacetamide (**6r**). White solid; yield: 33.87%; M.P.: 222–224 °C; IR (KBr)  $\nu$  (cm<sup>-1</sup>): 3303, 3205, 2920, 1677, 1078; <sup>1</sup>H NMR (400 MHz, DMSO-*d*<sub>6</sub>): δ10.42 (s, 1H, CONH), 9.67 (s, 1H, NH), 7.95 (d,  $J = 8.8$  Hz, 2H, Ar-H), 7.29 (d,  $J = 6.0$  Hz, 2H, Ar-H), 7.27 (s, 1H, Ar-H), 6.97 (t,  $J = 7.2$  Hz, 3H, Ar-H), 6.358 (s, 1H, Ar-H), 4.93 (s, 2H, OCH<sub>2</sub>), 2.27 (s, 6H, CH<sub>3</sub>); <sup>13</sup>C NMR (400 MHz, DMSO *d*<sub>6</sub>): δ167.63, 165.42, 160.68, 157.89, 156.33, 138.96, 129.17, 126.20, 123.40, 121.63, 115.10, 100.63, 67.20, 29.37, 20.05; LC-MS:  $m/z$  calculated for C<sub>20</sub>H<sub>19</sub>ClN<sub>4</sub>O<sub>2</sub>: 382.8; found: 383.4 [M+1]<sup>+</sup>, 385.3 [M+2]<sup>+</sup>.

4.1.5.19. 2-(4-Bromophenoxy)-*N*-(4-((4-fluorophenyl)amino)-6-methylpyrimidin-2-yl) acetamide (**6s**). White solid; yield: 40.24%; M.P.: 200–202 °C; IR (KBr)  $\nu$  (cm<sup>-1</sup>): 3251, 3168, 2995, 1672, 1056; <sup>1</sup>H NMR (400 MHz, DMSO-*d*<sub>6</sub>): δ10.24 (s, 1H, CONH), 9.47 (s, 1H, NH), 7.68 (d,  $J = 8.0$  Hz, 2H, Ar-H), 7.16 (d,  $J = 7.2$  Hz, 2H, Ar-H), 7.12 (d,  $J = 7.0$  Hz, 1H, Ar-H), 7.10 (t,  $J = 3.6$  Hz, 1H, Ar-H), 6.848 (t,  $J = 6.8$  Hz, 1H, Ar-H), 6.75 (d,  $J = 8.4$  Hz, 1H, Ar-H), 6.30 (s, 1H, Ar-H), 4.92 (s, 2H, OCH<sub>2</sub>), 2.23 (s, 3H, CH<sub>3</sub>); <sup>13</sup>C NMR (400 MHz, DMSO *d*<sub>6</sub>): δ167.46, 165.21, 160.88, 158.68, 157.81, 156.39, 136.29, 132.27, 121.57, 118.74, 116.97, 100.20, 67.97, 23.29; LC-MS:  $m/z$  calculated for C<sub>19</sub>H<sub>16</sub>BrFN<sub>4</sub>O<sub>2</sub>: 431.3; found: 433.3 [M+2]<sup>+</sup>.

4.1.5.20. *N*-(4-((2-fluorophenyl)amino)-6-methylpyrimidin-2-yl)-2-(*m*-tolylxy)acetamide (**6t**). White solid; yield: 35.73%; M.P.: 160–163 °C; IR (KBr)  $\nu$  (cm<sup>-1</sup>): 3253, 3195, 2956, 1679, 1064; <sup>1</sup>H NMR (400 MHz, DMSO-*d*<sub>6</sub>): δ10.30 (s, 1H, CONH), 9.26 (s, 1H, NH), 8.35 (s, 1H, Ar-H), 7.25 (t,  $J = 8.0$  Hz, 1H, Ar-H), 7.14 (t,  $J = 3.2$  Hz, 2H, Ar-H), 7.11 (d,  $J = 4.4$  Hz, 1H, Ar-H), 6.74 (d,  $J = 7.6$  Hz, 1H, Ar-H), 6.70 (s, 1H, Ar-H), 6.64 (d,  $J = 8.4$  Hz, 1H, Ar-H), 6.48 (s, 1H, Ar-H), 4.87 (s, 2H, OCH<sub>2</sub>), 2.26 (s, 6H, CH<sub>3</sub>); <sup>13</sup>C NMR (400 MHz, DMSO *d*<sub>6</sub>): δ167.84, 165.72, 161.38, 157.90, 156.39, 155.02,

138.83, 129.11, 127.11, 124.41, 121.53, 115.31, 111.26, 100.32, 67.24, 23.40, 21.06; LCMS:  $m/z$  calculated for C<sub>20</sub>H<sub>19</sub>FN<sub>4</sub>O<sub>2</sub>: 366.4; found: 367.4 [M+1]<sup>+</sup>.

4.1.5.21. 2-(3,5-Dimethylphenoxy)-*N*-(4-((2,3-dimethylphenyl)amino)-6-methylpyrimidin-2-yl)acetamide (**6u**). White solid; yield: 30.76%; M.P.: 198–200 °C; IR (KBr)  $\nu$  (cm<sup>-1</sup>): 3247, 3215, 2972, 1683, 1087; <sup>1</sup>H NMR (400 MHz, DMSO-*d*<sub>6</sub>): δ9.99 (s, 1H, CONH), 8.92 (s, 1H, NH), 7.15 (d,  $J = 7.6$  Hz, 2H, Ar-H), 7.08 (t,  $J = 7.6$  Hz, 1H, Ar-H), 7.02 (d,  $J = 7.2$  Hz, 1H, Ar-H), 6.56 (s, 1H, Ar-H), 6.43 (s, 2H, Ar-H), 6.03 (s, 1H, Ar-H), 4.82 (s, 2H, OCH<sub>2</sub>), 2.20 (s, 12H, CH<sub>3</sub>), 2.07 (s, 3H, CH<sub>3</sub>); <sup>13</sup>C NMR (400 MHz, DMSO-*d*<sub>6</sub>): δ168.57, 165.61, 162.69, 158.05, 156.81, 138.38, 137.37, 136.73, 132.31, 127.21, 125.58, 124.12, 122.30, 112.10, 98.13, 67.43, 23.37, 21.02, 20.09, 14.11; LC-MS:  $m/z$  calculated for C<sub>23</sub>H<sub>26</sub>N<sub>4</sub>O<sub>2</sub>: 390.5; found: 391.4 [M+1]<sup>+</sup>.

4.1.5.22. *N*-(4-((2,3-dimethylphenyl)amino)-6-methylpyrimidin-2-yl)-2-phenoxyacetamide (**6v**). White solid; yield: 30.28%; M.P.: 181–184 °C; IR (KBr)  $\nu$  (cm<sup>-1</sup>): 3215, 3126, 2929, 1687, 1076; <sup>1</sup>H NMR (400 MHz, DMSO-*d*<sub>6</sub>): δ10.09 (s, 1H, CONH), 8.95 (s, 1H, NH), 7.27 (t,  $J = 7.6$  Hz, 2H, Ar-H), 7.17 (d,  $J = 7.6$  Hz, 1H, Ar-H), 7.05 (d,  $J = 8.8$  Hz, 1H, Ar-H), 6.93 (t,  $J = 7.6$  Hz, 1H, Ar-H), 6.78 (d,  $J = 8.0$  Hz, 2H, Ar-H), 6.04 (s, 1H, Ar-H), 4.86 (s, 2H, OCH<sub>2</sub>), 2.22 (s, 6H, CH<sub>3</sub>), 2.08 (s, 3H, CH<sub>3</sub>); <sup>13</sup>C NMR (400 MHz, DMSO-*d*<sub>6</sub>): δ168.57, 165.61, 162.69, 158.05, 156.81, 139.38, 137.37, 132.31, 129.21, 126.12, 122.30, 114.10, 98.13, 67.43, 23.37, 20.09, 14.11; LC-MS:  $m/z$  calculated for C<sub>21</sub>H<sub>22</sub>N<sub>4</sub>O<sub>2</sub>: 362.4; found: 363.5 [M+1]<sup>+</sup>.

4.1.5.23. *N*-(4-((2,3-dimethylphenyl)amino)-6-methylpyrimidin-2-yl)-2-(4-fluorophenoxy) acetamide (**6w**). White solid; yield: 30.05%; M.P.: 187–190 °C; IR (KBr)  $\nu$  (cm<sup>-1</sup>): 3220, 3120, 2977, 1683, 1072; <sup>1</sup>H NMR (400 MHz, DMSO-*d*<sub>6</sub>): δ10.12 (s, 1H, CONH), 8.96 (s, 1H, NH), 7.17 (d,  $J = 7.6$  Hz, 1H, Ar-H), 7.1 (t,  $J = 3.2$  Hz, 2H, Ar-H), 7.03 (d,  $J = 7.2$  Hz, 2H, Ar-H), 6.80 (d,  $J = 4.4$  Hz, 2H, Ar-H), 6.04 (s, 1H, Ar-H), 4.84 (s, 2H, OCH<sub>2</sub>), 2.08–2.50 (s, 9H, CH<sub>3</sub>); <sup>13</sup>C NMR (400 MHz, DMSO-*d*<sub>6</sub>): δ168.57, 165.61, 162.69, 158.05, 156.81, 138.38, 136.73, 132.31, 127.21, 122.30, 116.12, 115.10, 98.13, 67.43, 23.37, 20.09, 14.11; LC-MS:  $m/z$  calculated for C<sub>21</sub>H<sub>21</sub>FN<sub>4</sub>O<sub>2</sub>: 380.4; found: 381.4 [M+1]<sup>+</sup>.

#### 4.2. Caspase-1 enzyme based assay

The potential ability of synthesized compound was determine using Caspase-Glo 1 Assay (10 ml) kit purchased from Promega (Cat.# G9951/2). Active recombinant human caspase-1 was obtained from Biovision (Cat.# 1081-100). The enzyme was diluted with 50  $\mu$ l of buffer, divided into 10  $\mu$ l aliquots, and stored at –20 °C. One unit (1pmol of AMC product formed/minute) diluted enzyme was used in the assay [25]. Caspase 1 buffer was prepared by dissolving (50 mM HEPES, 50 mM NaCl, 10 mM DTT, 0.1% CHAPS, 10 mM EDTA, 5% GLYCEROL) in 20 ml of distilled water. The Z-WEHD-AMC was reconstituted with a Caspase-Glo 1 buffer for yielding a final substrate concentration of 20  $\mu$ M in the assay. The Caspase-GloR 1 reagent was prepared by adding 3.0  $\mu$ l of MG-132 Inhibitor to 500  $\mu$ l of reconstituted Z-WEHD substrate for yielding a final concentration of 60  $\mu$ M in the assay. The peptide inhibitor Ac-YVAD-CHO was diluted at a ratio of 1:1000 (i.e., 0.25  $\mu$ l of Ac-YVAD-CHO Inhibitor diluted with 250  $\mu$ l Caspase-GloR 1 Reagent) to achieve the final concentration of 1  $\mu$ M per assay. Negative control (blank), positive control (enzyme controls), DMSO control and test compounds were assayed in triplicate in a 384-well plate. Initially 10  $\mu$ l (in negative control well), 8  $\mu$ l (in positive control well) and 3  $\mu$ l of buffer solution was added in experimental wells. After that 5  $\mu$ l of inhibitors were used in 100, 200 and 400

$\mu\text{M}$  concentrations (DMSO < 2%) and 3  $\mu\text{l}$  of enzyme was added in the experimental wells. Lastly 10  $\mu\text{l}$  of reconstituted Z-WEHD-AMC substrate was added in to each well, reaction content were mixed and incubated for 20 min. The accumulation of AMC was measured using Perkin Elmer, 2030 Multilabel Reader, VICTRO X3 [18]. The activity was calculated as AMC cleavage per min from the linear phase of the experiment. The  $\text{IC}_{50}$  values were calculated from dose response curve obtained by plotting % enzyme inhibition vs. concentration of test compounds using Prism<sup>TM</sup> 4 software (GraphPad).

#### 4.3. Cell based assay

A suspension of human monocytic cells (THP-1, ATCC code: TIB202,  $2 \times 10^6/\text{ml}$  in RPMI 1640 medium from Gibco BRL) was plated in 96-well plates, incubated and allowed to equilibrate at room temperature [19]. The negative, positive and test set compounds were assayed in triplicate manner. 100  $\mu\text{l}$  of Caspase-Glo1 reagent was added in each well and test set compounds were administered by concentrations range of 1  $\mu\text{M}$  to 100  $\mu\text{M}$ . Mixed all the reaction contents, incubate it for stabilizing the luminescent signal. The luminance was measure using Perkin Elmer, 2030 Multilabel Reader, VICTRO X3. The caspase-1 activity was accessed by comparing the results of treated cells with the untreated cells.

#### 4.4. Molecular docking

Docking study was performed using Grid-based Ligand Docking with Energetics software (GLIDE, Schro(ö)dinger, LLC, New York, 2009) [26]. The crystal structure of caspase-1,3,7 and 8 (PDB: 1RWX,1PAU,2QL9,1F9E) were retrieved from protein data bank and prepared (by removing water molecules, assigning bond orders and adding H-atoms) using *Protein Preparation Wizard (PPrep)* embedded in Maestro. The atom type was defined, charge state was optimized and protein structure was minimized using OPLS-2005 force field. The shape and properties of the receptor was represented by computing a grid box of  $20 \times 20 \times 20 \text{ \AA}$  at the centre of co-crystallized ligand using *Receptor Grid Generation Panel*. Subsequently, a stable ligand conformation was generated using the *LigPrep* and *ConfGen* tools of Schro(ö)dinger suite. The docking study of test compounds was carried out using extra precision (XP) mode of Glide. To soften the potential of nonpolar part of protein, the van derWaals scaling factor was kept at 1.0 with partial atomic charge cut-off of 0.25 and Coulomb-vdW cut-off of 50 kcal/mol. Scoring function estimates the energy-minimized poses and ranked by Glide scoring function (G-score) [27]. Finally, the docking poses of top-scored hits were visualized by Maestro 9.0 interface (Schro(ö)dinger Suite 9.0, NewYork, USA).

#### 4.5. Molecular dynamic simulations

Molecular dynamic (MD) simulation of protein-ligand complex was performed using *Desmond* module. The structural stability and influence of conserved water molecules was investigated by running this protocol for 30 ns. For MD simulation protein-ligand complex was saturated, partial charges were determined and energy was minimized using OPLS\_2005 force field of Schro(ö)dinger 2009 [28]. Topology and atomic coordinates of the complex was determined and immersed in to orthorhombic box  $10 \times 10 \times 10 \text{ \AA}$  of TIP3P solvent model including 11,599 water molecules. The system was neutralized by adding  $\text{Na}^+/\text{Cl}^-$  counter ions and salt concentration was maintained at 0.15 M. The H atoms were free to move during simulation. The NPT equilibration was ensemble under periodic boundary conditions using Nose-Hoover chain thermostat and Martyn-Tobias-Klein barostat. The system was

relaxed at 1 bar and 10 K and equilibrated at 300 K and 1 bar for a 30 ns. For long-range electrostatic interactions smooth particle mesh Ewald (PME) method was used; non-bonded van derWaals interactions were measured at cut-off distance of 10  $\text{Å}$  [29]. Most probable binding orientation of ligand within binding site of enzyme was described using simulation interaction diagram. The resulting trajectories were recorded at interval of 5.0 ns. Plots of RMSD, RMSF and hydrogen bonds were generated along with its dynamic simulation.

#### 4.6. ADME prediction

The absorption, distribution, metabolism and excretion (ADME) properties of the target compounds were predicted using *QikProp* module [22]. It predicts various ADME properties such as partition coefficient ( $Q\text{PlogPo/w}$ ), water solubility ( $Q\text{PlogS}$ ), cell permeability ( $Q\text{PPCaco-2}$ ), % human oral absorption and HERG  $\text{K}^+$   $\text{IC}_{50}$  ( $Q\text{PlogHERG}$ ). The physically and pharmaceutically significant properties of the molecules were predicted by “normal mode” with default setting.

#### Acknowledgement

The authors are thankful to Oxygen Healthcare Research Pvt. Ltd. Changodar, Ahmedabad for providing technical support for biological studies.

#### Conflicts of interest

The authors declare no conflict of interest about this article.

#### Appendix A. Supplementary material

Supplementary data associated with this article can be found, in the online version, at <https://doi.org/10.1016/j.bioorg.2018.03.019>.

#### References

- [1] D.R. McIlwain, T. Berger, T.W. Mak, Caspase functions in cell death and disease, Cold Spring Harb Perspect. Biol. 5 (2013) 1–28.
- [2] T. O'Brien, S.D. Linton, Design of Caspase Inhibitors as Potential Clinical Agents, first ed., CRC Press; Boca Raton, FL, USA, 2009, pp. 1–18.
- [3] A. Degterev, M. Boyce, J. Yuan, A decade of caspases, Oncogene 22 (2003) 8543–8567.
- [4] A. Denes, G. Lopez-Castejon, D. Brough, Caspase-1: is IL-1 just the tip of the ICEberg?, Cell Death Disease 338 (2012) 1–9.
- [5] C.A. Dinarello, Interleukin-1 in the pathogenesis and treatment of inflammatory diseases, Blood 117 (2011) 3720–3732.
- [6] S.M. Allan, P.J. Tyrrell, N.J. Rothwell, Interleukin-1 and neuronal injury, Nat. Rev. Immunol. 5 (2005) 629–640.
- [7] J.C. Randle, M.W. Harding, G. Ku, M. Schonharting, R. Kurrle, ICE/Caspase-1 inhibitors as novel anti-inflammatory drugs, Expert Opin. Investig. Drugs 10 (2001) 1207–1209.
- [8] D.S. Hallegua, M.H. Weisman, Potential therapeutic uses of interleukin 1 receptor antagonists in human diseases, Ann. Rheum. Dis. 61 (2002) 960–967.
- [9] L.D. Church, M.F. McDermott, Canakinumab, a fully-human mAb against IL-1beta for the potential treatment of inflammatory disorders, Curr. Opin. Mol. Ther. 11 (2009) 81–89.
- [10] M. Garcia-Calvo, E.P. Peterson, B. Leiting, R. Ruel, D.W. Nicholson, N.A. Thornberry, Inhibition of human caspases by peptide-based and macromolecular inhibitors, J. Biol. Chem. 273 (1998) 32608–32613.
- [11] B. Siegmund, M. Zeitz, Pralnacasan(vertex pharmaceuticals), IDrugs 6 (2003) 154–158.
- [12] J.H. Stack, K. Beaumont, P.D. Larsen, K.S. Straley, G.W. Henkel, J.C. Randle, IL-converting enzyme/caspase-1 inhibitor VX-765 blocks the hypersensitive response to an inflammatory stimulus in monocytes from familial cold autoinflammatory syndrome patients, J. Immunol. 175 (2005) 2630–2634.
- [13] T. O'Brien, B.T. Fahr, M.M. Sopko, J.W. Lam, N.D. Waal, B.C. Raimundo, H.E. Purkey, P. Pham, M.J. Romanowski, Structural analysis of caspase-1 inhibitors derived from Tethering, Acta Cryst. F 61 (2005) 451–458.
- [14] A.V. Erkin, V.I. Krutikov, Synthesis and molecular structure of 1-(pyrimidin-2-yl)-2-(4-aryl-1,3-thiazol-2-yl)hydrazines, Russ. J. Gen. Chem. 81 (2011) 1699–1704.

- [15] M.T. Chhabria, H.G. Bhatt, H.G. Raval, P.M. Oza, Synthesis and biological evaluation of some 5-ethoxycarbonyl-6-isopropylamino-4-(substitutedphenyl) aminopyrimidines as potent analgesic and anti-inflammatory agents, *Bioorganic Med. Chem. Lett.* 17 (2007) 1022–1024.
- [16] R.J. Altenbach, R.M. Adair, B.M. Bettencourt, L.A. Black, S.R. Fix-Stenzel, S.M. Gopalakrishnan, G.C. Hsieh, H. Liu, K.C. Marsh, M.J. McPherson, I. Milicic, T.R. Miller, T.A. Vortherms, U. Warrior, J.M. Wetter, N. Wishart, D.G. Witte, P. Honore, T.A. Esbenshade, A.A. Hancock, J.D. Brioni, M.D. Cowart, Structure–Activity Studies on a Series of a 2-Aminopyrimidine-Containing Histamine H<sub>4</sub> Receptor Ligands, *J. Med. Chem.* 51 (2008) 6571–6580.
- [17] S. Valente, Y. Liu, M. Schnekenburger, C. Zwergel, S. Cosconati, C. Gros, M. Tardugno, D. Labella, C. Florean, S. Minden, H. Hashimoto, Y. Chang, X. Zhang, G. Kirsch, E. Novellino, P.B. Arimondo, E. Miele, E. Ferretti, A. Gulino, M. Diederich, X. Cheng, A. Mai, Selective non-nucleoside inhibitors of human DNA methyltransferases active in cancer including in cancer stem cells, *J. Med. Chem.* 57 (2014) 701–713.
- [18] M. O'Brien, D. Moehring, R. Munoz-Planillo, G. Nunez, J. Callaway, J. Ting, M. Scurria, T. Ugo, L. Bernad, J. Cali, D. Lazar, A bioluminescent caspase-1 activity assay rapidly monitors inflammasome activation in cells, *J. Immunol. Methods.* 447 (2017) 1–13.
- [19] H. Ahn, G.-S. Lee, Isorhamnetin and hyperoside derived from water dropwort inhibits inflammasome activation, *Phytomedicine* 24 (2017) 77–86.
- [20] Y. Wei, T. Fox, S.P. Chambers, J. Sintchak, J.T. Coll, J.M.C. Golec, L. Swenson, K.P. Wilson, P.S. Charifson, The structures of caspases-1, -3, -7 and -8 reveal the basis for substrate and inhibitor selectivity, *ACS Chem. Biol.* 7 (2000) 423–432.
- [21] R. Mehra, R. Chib, G. Munagala, K.R. Yempalla, I.A. Khan, P.P. Singh, F.G. Khan, A. Nargotra, Erratum to: discovery of new Mycobacterium tuberculosis proteasome inhibitors using a knowledge-based computational screening approach, *Mol. Divers.* 20 (2016) 367.
- [22] QikProp, version 4.3, Schro(ö)dinger, LLC, New York, NY, 2015.
- [23] G. Nagy, S.V. Filip, E. Surducan, V. Surducan, Solvent-free synthesis of substituted phenoxyacetic acids under microwave irradiation, *Synth. Commun.* 27 (1997) 3729–3736.
- [24] M.J. Aaglawe, S.S. Dhule, S.S. Bahekar, P.S. Wakte, D.B. Shinde, Synthesis and antibacterial activity of some oxazolone derivatives, *J. Korean Chem. Soc.* 47 (2003) 133–136.
- [25] H.-Y. Kim, S.-Y. Nam, J.-B. Jang, Y. Choi, I.-C. Kang, H.-M. Kim, H.-J. Jeong, 2-(4-[(phenylthio)acetyl]carbonohydrizonoyl)phenoxy)acetamide as a new lead compound for management of allergic rhinitis, *Inflamm. Res.* 65 (2016) 963–973.
- [26] L. Chen, L. Wang, Q. Gu, J. Xu, An in silico protocol for identifying mTOR inhibitors from natural products, *Mol. Divers.* 18 (2014) 841–852.
- [27] T.A. Halgren, R.B. Murphy, R.A. Friesner, H.S. Beard, L.L. Frye, W.T. Pollard, J.L. Banks, Glide: a new approach for rapid, accurate docking and scoring. 2. Enrichment factors in database screening, *J. Med. Chem.* 47 (2004) 1750–1759.
- [28] D. Shivakumar, J. Williams, Y. Wu, W. Damm, J. Shelley, W. Sherman, Prediction of absolute solvation free energies using molecular dynamics free energy perturbation and the OPLS force field, *J. Chem. Theory Comput.* 6 (2010) 1509–1519.
- [29] U. Deniz, E. Ozkirimli, K.O. Ulgen, A systematic methodology for large scale compound screening: a case study on the discovery of novel S1PL inhibitors, *J. Mol. Graph Model.* 63 (2016) 110–124.